

# Solvent cast thermoplastic and thermoset rigid-rod molecular composites

N. Venkatasubramanian<sup>a</sup>, D.R. Dean<sup>b,1</sup>, T.D. Dang<sup>b</sup>, G.E. Price<sup>c</sup>, F.E. Arnold<sup>b,\*</sup>

<sup>a</sup>Systran Federal Corporation, 4126, Linden Avenue, Dayton, OH 45432, USA

<sup>b</sup>Polymer Branch, AFRL/MLBP, Materials Directorate, Wright Laboratory, 2941, P Street, Suite 1, Wright-Patterson Air Force Base, OH 45433-7750, USA

<sup>c</sup>University of Dayton Research Institute, 300 College Park, Dayton, OH 45469, USA

Received 9 February 1999; received in revised form 24 June 1999; accepted 15 July 1999

## Abstract

Acid–base interaction-mediated compatibilization between rigid-rod and matrix polymer components facilitated the formation and processing of solvent cast aromatic heterocyclic rigid-rod thermoplastic as well as thermoset molecular composites above the critical concentration ( $C_{cr}$ ) of the rigid-rod polymer in solution, without phase separation. The blends were solvent cast by the mechanism of ionic interchange between a sulfonic acid-pendent poly(*p*-phenylenebenzobisimidazole) (SPBI), solubilized in alcohol as its triethylammonium salt and basic thermoplastics such as poly(vinylpyridine)s or secondary or tertiary amines with thermosettable phenylethynyl, nadimide and bisbenzoxazine functionalities. Morphological characterization, utilizing SEM, WAXS and SAXS of as cast as well as annealed/thermally cured optically clear film composites of a broad range of compositions revealed homogeneous microstructures with no observable phase-separated domains, indicating high miscibility, ascribable to the favorable negative enthalpy of the ionic association between the rod-matrix components. A preliminary dynamic mechanical study of compression molded rigid-rod thermoplastic blends with relatively low rod contents showed significant enhancement in thermomechanical properties vis-à-vis the pristine matrix. © 2000 Elsevier Science Ltd. All rights reserved.

**Keywords:** Rigid-rod thermoplastic molecular composite; Rigid-rod thermoset molecular composite; Acid–base interaction-mediated compatibilization

## 1. Introduction

A relatively new concept in materials technology, the rigid-rod molecular composite has been the subject of extensive research interest since its inception. It is defined as the molecular dispersion of a rigid-rod polymer in a flexible coil polymer matrix such that the rods act as the reinforcing elements [1]. The proof of concept and the fabrication of the first true rigid-rod molecular composite were initially demonstrated [2] using poly(*p*-phenylenebenzobisthiazole) (PBT) as the rigid-rod reinforcement and poly(2,5(6)benzimidazole) (ABPBI) as the continuous semi-flexible coil matrix phase. To ensure the molecular dispersity of the rigid-rod polymer in the blend, the processing of the composite could only be carried out from solutions at lower than its critical concentration  $C_{cr}$  (3–4 vol%) [3] to prevent the segregation of the rigid-rod reinforcement. Above  $C_{cr}$  the solutions became biphasic where the rigid-rod segregated into liquid crystalline (lyotropic) domains which were dispersed in an entangled flexible coil matrix and the desired

mechanical performance of the composite was not realized. Since in this model system the rod as well as the matrix polymers did not possess glass transition temperatures for subsequent post-form consolidation, thermoplastic matrix polymers such as nylons, polyphenylquinoxaline and polyetheretherketone were used as the host matrix, the rigid-rod reinforcement being PBT [4–6]. The two major disadvantages encountered in these polymer blend systems were the occurrence of thermally induced phase separation during consolidation and the limited choice of thermoplastic matrix polymers based on their solubility as well as stability in strong, corrosive acids such as methanesulfonic acid (MSA).

Though not as extensively investigated as rod-thermoplastic molecular composites, there are a limited number of reports dealing with issues related to phase separation of the rods in solution processed rigid-rod thermoset molecular composites [7–10]. A study of the composite involving PBT and a benzocyclobutene (BCB) thermosetting oligomer as host matrix showed a spherical domain structure of the thermoset due to phase separation [8]. Whereas an increased entanglement in the form of a high molecular weight aromatic polyamide matrix with a crosslinkable benzocyclobutene pendant [9,10] showed that the degree

\* Corresponding author.

<sup>1</sup> Present address: Center for Advanced Materials, 331 Chappie James Building Tuskegee University, Tuskegee, AL 36088, USA.

of phase separation in the coagulated composite of the PBT/thermosetting polymer was significantly smaller than that in the PBT/BCB oligomer composite, it did not overcome the problem.

A number of approaches have been made in our laboratories and elsewhere to circumvent phase separation during the processing of a variety of molecular composite systems and has recently been reviewed [6]. One of the recent approaches to overcome the thermodynamic driving force for phase separation in polymer blends is to promote miscibility between specifically modified polymer components via ion–ion, acid–base [11,12] and ion–dipole [13,14] interactions. The initial promise of an ionic rigid-rod molecular composite [15] formed between a polyelectrolyte host and the reinforcing rigid-rod polymer PBT was demonstrated in a coagulated blend system, processed below  $C_{cr}$  of the rigid-rod polymer in methanesulfonic acid.

In this paper, we report an acid–base interaction-mediated approach to the formation and processing of an aromatic heterocyclic rigid-rod thermoplastic as well as a thermoset molecular composite, above  $C_{cr}$  of the rigid-rod polymer, to a degree at which the polymer blend can be cast from solution. A series of rigid-rod benzobisazole polymers functionalized with pendent sulfonic acid groups have been synthesized in our laboratories [16–18]. These sulfo-pendent rigid-rods can form an ionic association with polar thermoplastic matrix polymers with a basic functionality or with basic thermoset matrix molecules providing a mechanism by which miscibility can be promoted between the two components and thus phase separation during the processing of the molecular composite can be prevented even above  $C_{cr}$  of the rod. The mixture of the two components is expected to behave as one via this specific interaction and therefore can be cast from solution. In the current study, cast films of such composites were obtained and found to be planar isotropic and optically clear. This can be attributed to the repulsion between ionically charged rigid-rod molecules, thus precluding aggregation of the rods leading to phase separation in the matrix.

The aromatic heterocyclic rigid-rod polymer system chosen as the reinforcing element in the molecular composite was poly[(1,7-dihydrobenzo[1,2-d:4,5-d']diimidazo-2,6-diyl)-2-(2-sulfo)-*p*-phenylene] (SPBI) which could be solubilized as its triethylammonium salt in methanol. The thermoplastic materials investigated for the formation of the blends were poly(4-vinylpyridine) (PVP) and poly(2-vinylpyridine) and the thermosetting matrix materials in this study comprised secondary amines with thermosettable phenylethynyl and nadimide functionalities ([iminobis(*N*-propyl-2-phenylethynylphthalimide)] and [iminobis(*N*-propyl nadic imide)], respectively) [19] and a thermoset with two tertiary amine functionalities, the bis-*N*-methylbenzoxazine thermosetting monomer derived from bisphenol A [2,2-bis(3,4-dihydro-3-methyl-2H-1,3-benzoxazine)propane] [20,21]. This paper describes the formation of such solvent cast rigid-rod molecular composite

films with particular emphasis on the morphological characterization of as cast as well as annealed/thermally cured molecular composites. In the case of the thermoplastic rigid-rod molecular composites, thermally consolidated blends were also investigated from the point of view of morphology and thermal properties.

## 2. Experimental

### 2.1. Materials

The sulfo-pendent rigid-rod polymer SPBI was synthesized as reported previously [16,17]. In the current study, two batches of SPBI with intrinsic viscosity (IV) of 4.0 and 7.0 dl/g (in methanesulfonic acid at 30°C) were used as the reinforcing rigid-rod polymer component. The thermoplastics poly(4-vinylpyridine) (PVP, MW 200,000, reported  $T_g$  158°C) and poly(2-vinylpyridine) (MW 200,000, reported  $T_g$  104°C) were purchased from Specialty Polymer Products. The thermosetting secondary amines with phenylethynyl and nadimide functionalities, synthesized as reported [19], were available in the Air Force Materials Laboratories. The bisphenol A-derived benzoxazine thermoset was received from Prof. Ishida, Department of Macromolecular Science, Case Western Reserve University, Cleveland, OH and used without further purification. Anhydrous methanol, anhydrous *N,N*-dimethylacetamide (DMAc) and triethylamine were purchased from Aldrich Chemicals and used as such.

### 2.2. Solubilization of the sulfo-pendent rigid-rod

The sulfo-pendent rigid-rod, SPBI was solubilized as its triethylammonium salt in methanol. SPBI (0.30 g) (IV = 4.0 dl/g) was suspended in 300 ml anhydrous methanol and a large excess (4.0 g) of triethylamine was added to the red suspension. Dissolution of the polymer started to occur and the solubilization was completed under methanol reflux conditions in a dry nitrogen atmosphere overnight. A clear, greenish yellow solution of the triethylammonium salt of SPBI in methanol was obtained. Various volumes of the 0.10 wt% polymer solution were used for the formation of the thermoplastic rigid-rod blend film compositions described in this study. This was also used for the processing of a cast SPBI film via sulfo-reversion (volatilization of triethylamine from the organic ammonium salt of SPBI to regenerate the sulfonic acid form).

SPBI (0.50 g) (IV = 7.0 dl/g) was suspended in 300 ml anhydrous methanol and with the addition of triethylamine (4.0 g), instant solubilization of the polymer in methanol was observed. The greenish yellow solution was refluxed overnight under a dry nitrogen atmosphere to complete the dissolution. This solution (0.16 wt% polymer) was used in the formation of thermoset rigid-rod blend film compositions as well as precipitated thermoplastic rigid-rod blend compositions which were thermally consolidated by compression molding for dynamic mechanical analysis.

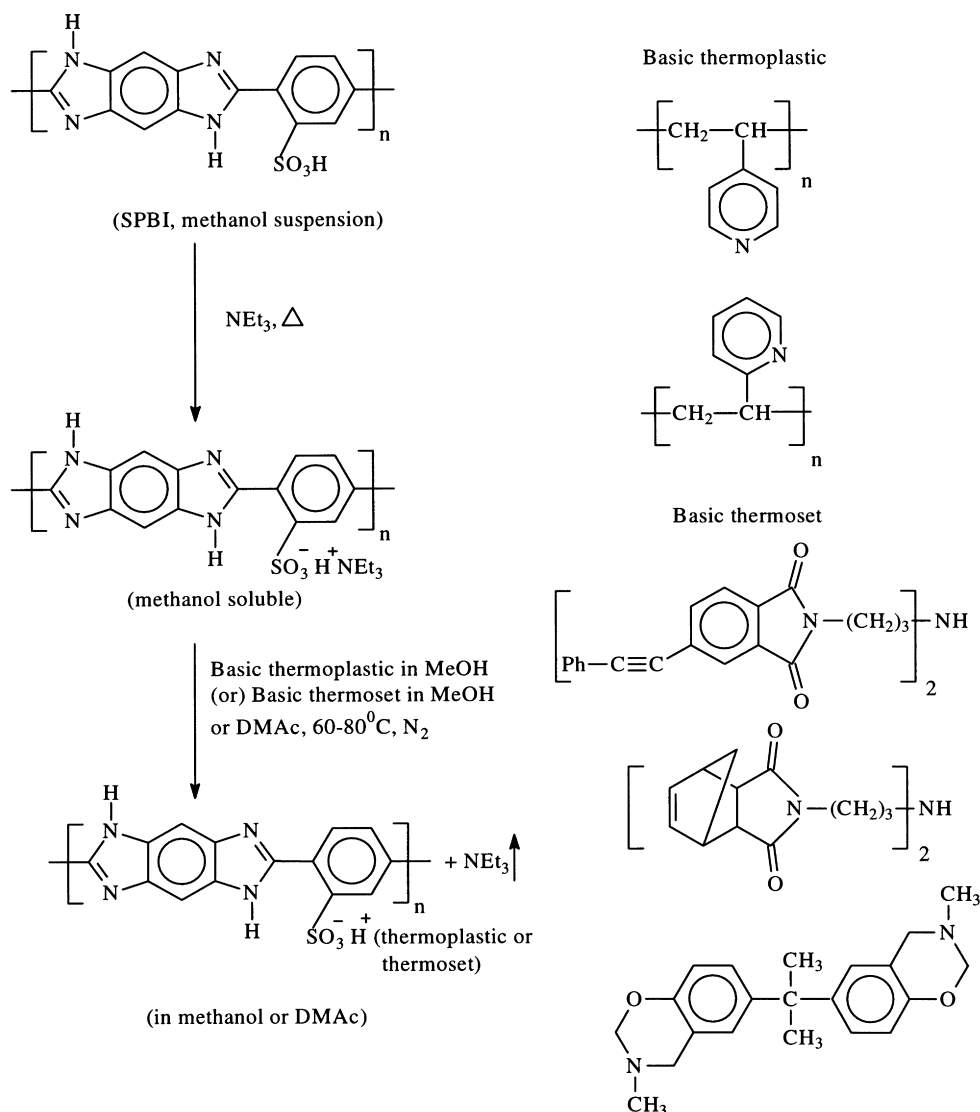


Fig. 1. Formation of rigid-rod thermoplastic and thermoset molecular composites via ionic interchange.

### 2.3. Formation of the rigid-rod thermoplastic polymer blends

A representative example for the formation of rigid-rod thermoplastic molecular composite films is described below.

#### 2.3.1. Molecular composite film from SPBI and PVP with 50/50 (w/w) rod/coil composition

To 25 ml methanolic solution of the triethylammonium salt of SPBI (0.025 g of the polymer) was added 10 ml methanolic solution containing 0.025 g PVP. The mixture was vigorously stirred in a three-necked flask fitted with an inlet and an outlet for passage of dry nitrogen. The homogeneous, greenish yellow solution was heated on an oil bath in the temperature range 60–80°C for several hours, driving off the volatile methanol and triethylamine; dry methanol was intermittently added during the process to prevent the

solution from gelling. The blend in methanol was concentrated to a viscous solution, which was transferred to a glass casting dish; the solvent was then evaporated in a vacuum hood overnight, leaving behind a transparent yellowish orange film composite with a 50/50 (w/w) rod/coil composition.

Aggregated rod/coil molecular composites (5/95, 10/90 and 20/80 (w/w) rod/coil) were obtained by precipitation of the blend from a viscous methanolic solution by the addition of water as non-solvent. An example is given below.

#### 2.3.2. Aggregated molecular composite from SPBI and PVP with 5/95 (w/w) rod/coil composition

To 10 ml methanolic solution of the triethylammonium salt of SPBI containing 0.0166 g of the sulfonic acid polymer was added 0.3166 g of PVP in 20 ml methanol. The yellow solution was heated under a nitrogen purge on an oil bath at 80°C to facilitate evaporation of both methanol

Table 1  
Methanol cast aromatic heterocyclic rigid-rod (SPBI) thermoplastic molecular composites

Polymer matrix	Composition (rod/coil, w/w)	Film appearance
Poly(4-vinylpyridine)	10/90	Clear, yellow
Poly(4-vinylpyridine)	20/80	Clear, yellow
Poly(4-vinylpyridine)	50/50	Clear, yellowish orange
Poly(4-vinylpyridine)	75/25 <sup>a</sup>	Clear, orange
Poly(2-vinylpyridine)	50/50	Clear, yellow
–	100/0	Clear, reddish orange

<sup>a</sup> This wt composition corresponds to acid–base molar equivalence of the rod and the matrix.

and triethylamine. Methanol was added intermittently to prevent the concentrated solution from gelling, keeping the polymer blend in a homogeneous solution. After several hours, the condensate from the solution was free of the triethylamine base (pH indicator). The solution was concentrated further and the viscous solution was pipetted out into a large excess of de-ionized, distilled water to precipitate the polymer blend as a fine suspension. After filtration using a 10–20  $\mu\text{m}$  fritted funnel, the composite was Soxhlet extracted with boiling water for 48–72 h and finally dried in vacuum at 100°C for 48 h to provide a dry, yellow fibrous composite specimen. The weight of the recovered, dried sample was 0.260 g.

#### 2.4. Formation of the rigid-rod thermoset molecular composite films

The general procedure consisted of the following. To the stirred alcoholic solution of the triethylammonium salt of SPBI was added a solution of the amine thermoset monomer in methanol or DMAc and the solution was heated under nitrogen to 60°C, allowing for the volatilization of

triethylamine. The viscous polymer solution was transferred to a casting dish and the solvents were evaporated (under high vacuum at room temperature for 72 h in a vacuum desiccator in the case of DMAc) to obtain composite films. The orange-colored film composites were optically clear, tough and flexible and the compositions, in general, corresponded to 1:1 molar ratio based on the interacting acid–base functionalities in the rod-thermoset matrix monomer components.

#### 2.5. Structure and morphology

Fourier transform infrared spectra (FTIR) of the samples were recorded on a Bruker IFS 28 FTIR spectrometer as polymer films and as KBr pellets for the thermoplastic/thermoset powders. Composite microstructure (as films or as thermally consolidated samples) was examined by scanning electron microscopy (SEM), Wide angle X-ray scattering (WAXS) and small angle X-ray scattering (SAXS). Scanning electron micrographs were taken using a JEOL-840 scanning electron microscope. For higher resolution micrographs, a Hitachi S-900 low-voltage, high resolution SEM

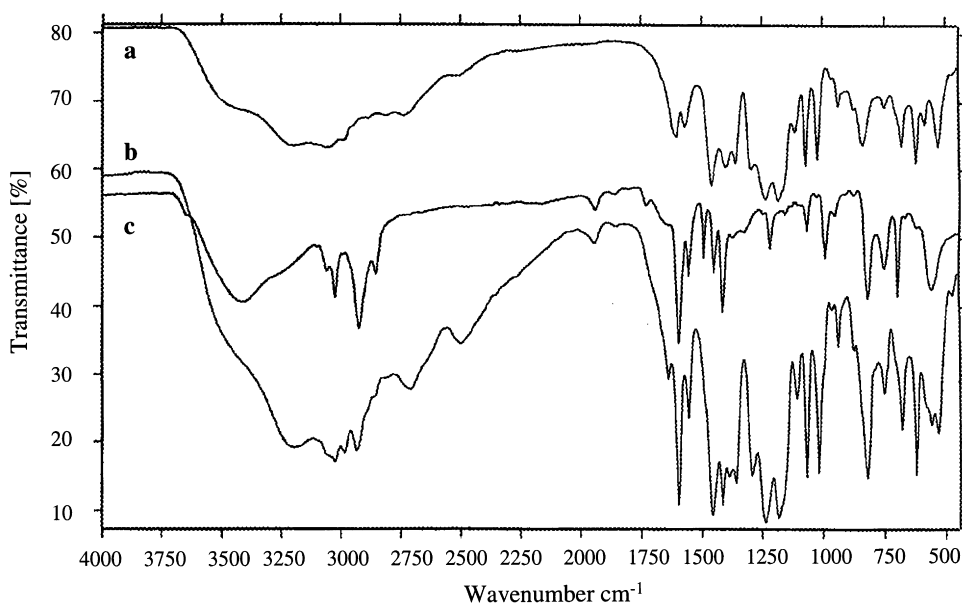


Fig. 2. IR spectra of: (a) cast SPBI film; (b) 50/50 (w/w) SPBI/PVP composite film; and (c) KBr disk of PVP.

Table 2  
Solvent (methanol or *N,N*-dimethylacetamide) cast aromatic heterocyclic rigid-rod (SPBI) thermoset molecular composites

Thermoset	Molar ratio (rod/thermoset)	Composition (rod/thermoset) (w/w)	Film appearance
Phenylethynyl	1/1	36/64	Clear, orange
Nadimide	1/1	42/58	Clear, orange
Nadimide	1/3	20/80	Clear, light orange
Benzoxazine	1/1	48/52	Clear, orange

was used. Fracture surfaces were prepared by immersing the films in liquid nitrogen prior to fracture. WAXS and SAXS measurements were performed using a Rigaku RU 200 or 300 rotating anode generator equipped with a Statton camera. The sample-to-film distance was varied to permit either WAXS or SAXS measurements. Nickel filtered  $\text{CuK}\alpha$  ( $\lambda = 1.5418 \text{ \AA}$ ) radiation was used at an accelerating voltage of 50 kV/170 mA. WAXS patterns were also obtained on phosphor image plates. WAXS plots were obtained after digitizing image plate data. Dynamic mechanical analysis (DMA) was performed using a Perkin–Elmer DMA 7 instrument. The compression-molded samples were tested in the flexural mode in DMA experiments, using a three-point bend fixture. The sample geometry was a small rectangular bar with a length of 15 mm, width of 3 mm and thickness of 1 mm. An oscillating frequency of 1 Hz and a temperature scanning rate of  $5^\circ\text{C}/\text{min}$  were used.

### 3. Results and discussion

#### 3.1. Formation of rigid-rod molecular composites

The formation of the cast rigid-rod thermoplastic as well as the thermoset composite via the mechanism of ionic interchange is schematically depicted in Fig. 1. Acid–base interaction between SPBI and the basic thermoplastic PVP or poly(2-vinylpyridine) in methanol was facilitated by the volatilization of the excess triethylamine base present in the solution as well as the triethylamine liberated by the decomposition of the organic ammonium salt of SPBI. The thermoset monomers with secondary and tertiary amine functionalities were compatibilized with SPBI and the blends solvent cast via the same mechanism from methanol or DMAc solutions.

Optically clear, homogeneous, cast film composites were obtained by this process and in the case of the thermoplastic composites, the rod-matrix coil miscibility was observed in the entire range of compositions of the two polymer components. The various film compositions are described in Table 1. Fig. 2 shows the IR spectra of a cast film of SPBI obtained via the sulfo-reversion process from its triethylammonium salt, a cast film of SPBI/PVP (50/50 (w/w) blend) and a KBr disk of PVP powder. SPBI shows aromatic and heteroaromatic stretches in the region  $1607\text{--}1462 \text{ cm}^{-1}$ , the asymmetric and symmetric S=O stretching frequencies in the  $1235\text{--}1116 \text{ cm}^{-1}$  range due to the hydrated sulfonic acid function and a broad OH band due to the sulfonic acid in the  $3500\text{--}2500 \text{ cm}^{-1}$  region. The aliphatic C–H stretch of the polyvinyl backbone of the thermoplastic at  $2925 \text{ cm}^{-1}$  is clearly discernible in the IR spectrum of the rod/coil blend.

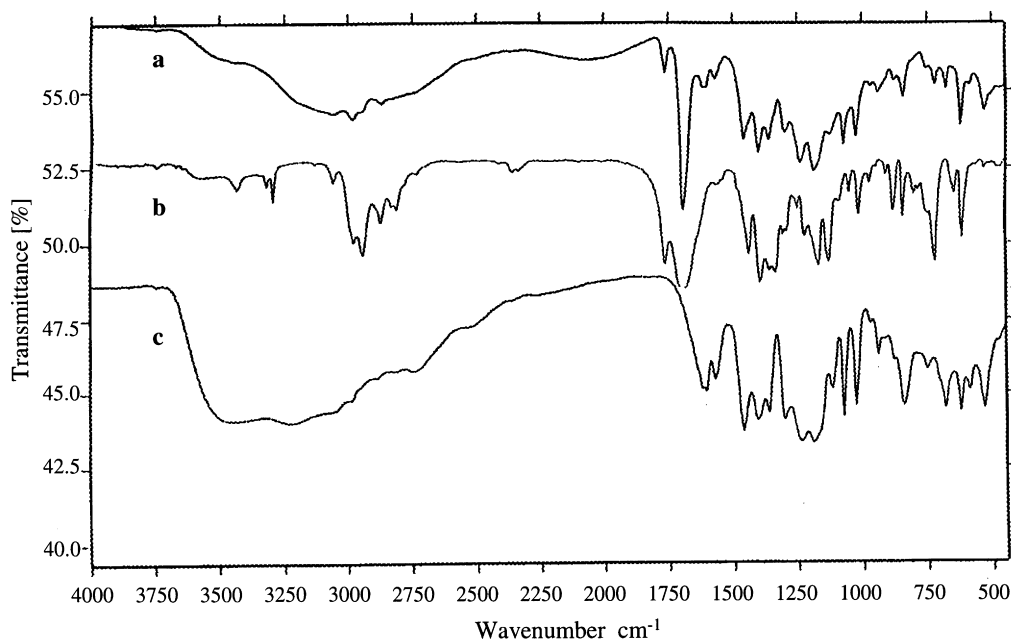


Fig. 3. IR spectra of: (a) cast 42/58 (w/w) SPBI/nadimide composite film; (b) KBr disk of the nadimide thermoset monomer; and (c) cast SPBI film.

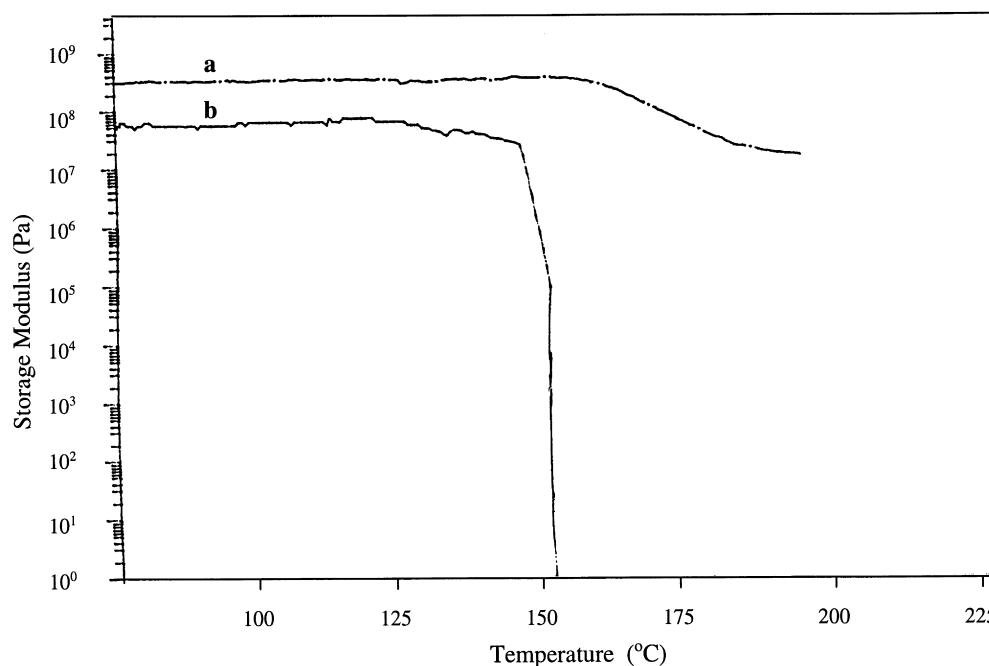


Fig. 4. DMA data for: (a) 5/95 (w/w) SPBI/PVP compression molded composite; and (b) compression molded PVP.

The broad band in the IR of the composite film extending from 3000 to 2000  $\text{cm}^{-1}$  arises due to the N–H stretch of the pyridinium function of the thermoplastic due to ionic association with the sulfonic acid of the rod.

Homogeneous, optically clear film composites were obtained for thermoset weight compositions that corresponded to or even exceeded a molar equivalence relative to the sulfonic acid functionality of the SPBI. The color of the composite films ranged from light orange to deep orange while a cast thin film of SPBI film was reddish orange. The various film compositions are listed in Table 2. The FTIR spectra of the cast transparent molecular composite film of SPBI/nadimide thermoset (1/1 rod/thermoset molar ratio or 42/58 (w/w) rod/thermoset), a cast SPBI film and a KBr disk of the nadimide thermosetting monomer are shown in Fig. 3. The spectrum of the composite structure exhibits the doublet at 1770 and 1700  $\text{cm}^{-1}$  characteristic of the nadimide functionality and the C–H stretch in the 2800–2980  $\text{cm}^{-1}$  region due to the aliphatic function in the thermoset amine monomer. The broad IR absorption encompassing 3500–2500  $\text{cm}^{-1}$  range precludes clear identification of N–H stretch that might arise due to protonation of the secondary amine functionality in the thermoset due to the sulfonic acid pendant in SPBI.

Aggregated rod/coil blends were also obtained for various compositions of the rod and the coiled matrix PVP by precipitation from the viscous methanolic solution of the polymer blend by the addition of a suitable non-solvent such as water. Blends with low rod/coil ratios were thermally consolidated into rectangular bars above the  $T_g$  of the thermoplastic matrix in the polymer blend. The enhancement of the  $T_g$  of the compression molded composite specimens

vis-à-vis the  $T_g$  of PVP was investigated as a function of the incorporation of the rod in the host polymer matrix.

### 3.2. Thermal characteristics of compression molded composites

Dynamic mechanical analysis (DMA) of compression molded composite samples was performed to evaluate the effects of specific interaction on the thermomechanical properties of the polymer matrix. The dynamic mechanical analysis experiments we conducted involved applying an oscillatory stress to the sample and measuring the resultant strain. The phase difference and the amplitudes of the stress and the strain waves are used to determine both the in-phase and the out-of-phase components of the modulus. The in-phase elastic component,  $E'$ , is the storage modulus while the out-of-phase viscous component,  $E''$ , is the loss modulus.

A rigid-rod thermoplastic molecular composite with relatively low rod content (5/95 (w/w) SPBI/PVP) was examined by DMA for comparison with compression molded PVP. The results are displayed as storage modulus vs. temperature plots for the 5/95 (w/w) rod/coil composite and pure PVP (Fig. 4). It can be seen from the plot that the storage modulus has increased by a factor of 6 as a result of the incorporation of the rod in the PVP matrix; additionally, the decrease in  $E'$  is found to occur in a significantly higher glass transition region for the 5/95 rod/coil composite compared to the pure thermoplastic. Also evident from the figure is a distinct broadening of the relaxation behavior of the rod-dispersed matrix composite relative to the pure, amorphous matrix. It is well known that the detection of a

Table 3

Glass transition temperatures of compression molded (at 195°C and 21 MPa for PVP, 210°C and 35 MPa for 5/95 (w/w) SPBI/PVP and 220°C and 35 MPa for 10/90 SPBI/PVP) SPBI/PVP composites

Rod/thermoplastic (w/w)	Measured $T_g^a$ (°C)
0/100	153
5/95	176
10/90	210

<sup>a</sup> From  $\tan \delta$  maxima in DMA.

single concentration-dependent  $T_g$  of the blend in which both components are thermoplastic is indicative of miscibility of blend domains less than 15 nm [22–24]. However, in our case the rigid-rod polymer does not exhibit a  $T_g$  prior to decomposition. Presumably, the presence of the sulfonic acid pendant does not change the rod-like nature of the poly(*p*-phenylenebenzobisimidazole) backbone. Even versions of this polymer derivatized with ionic propane sulfonate pendants did not exhibit a  $T_g$  and were found to form lyotropic solutions at relatively high concentrations [25]. In contrast to our findings, Hara and Parker [22]

have observed a  $T_g$  for the extended-rod poly(*p*-phenylene-terephthalamide) derivatized with ionic propane sulfonate and non-ionic propyl groups. They attribute this to the elimination of hydrogen bonding when the amide hydrogens are replaced by alkyl chains.

From the foregoing discussion, it is evident that the DMA data shown in Fig. 4 do not provide direct proof of miscibility of the rod-coil polymer components as compared to a blend system of two thermoplastics. However, the significant enhancement in the thermomechanical behavior of the blend due to as low as 5 wt% dispersion of the rigid-rod in the matrix is definitely indicative of miscibility of the two polymers, attributable to the specific interactions occurring between the two. Table 3 further describes the values of the measured glass transition temperature, obtained as an approximation from  $\tan \delta$  maxima in DMA, as a function of the rod content in compression molded SPBI/PVP composites. An increase in the  $T_g$  of the matrix from 153 to 210°C was observed upon incorporation of 10 wt% SPBI in PVP, again indicative of a well-defined synergistic effect due to strong intermolecular interactions between the rod and the matrix polymer components.

### 3.3. Morphology of thermoplastic rigid-rod molecular composites

#### 3.3.1. Scanning electron microscopy

SEMS of both the free surface and the fracture surface of the SPBI film are shown in Fig. 5. While the surface is essentially featureless, the fracture surface reveals a finely striated morphology with the striation ca. 0.1  $\mu\text{m}$  (100 nm) in width. This SEM morphology is significantly different from that reported for films of other rigid-rod polymers [2,26,27] in which well-defined platelet-like lamellar structures were obtained which seemed to have little or no inter-lamellar connections. Fracture surfaces of 10/90 (w/w) SPBI/PVP films, as cast and heat-treated, are shown in Fig. 6. The films show no evidence of phase separation on the scale probed by SEM (ca. 20 nm); although there is some texture visible, there are no distinct domains or domain boundaries as were reported by Krause et al. [27] for physically blended composites of PBT and ABPBI. In that work, when blends were processed from a solution in which the total polymer concentration was greater than the critical concentration, large-scale phase separation occurred with 0.1–4  $\mu\text{m}$  ellipsoidal particles of the rod-like polymers forming within the ductile matrix. Here we observe more of a co-continuous microstructure, indicative of good miscibility. The small holes that are visible at random locations are presumably artifacts that were formed by solvent evaporation during film formation.

It should be noted that Krause et al. [27] observed no evidence of phase separation by SEM in extruded films of PBT/ABPBI in which the total polymer concentration was less than the critical concentration. This particular case was very similar to our observation of the film morphology in the

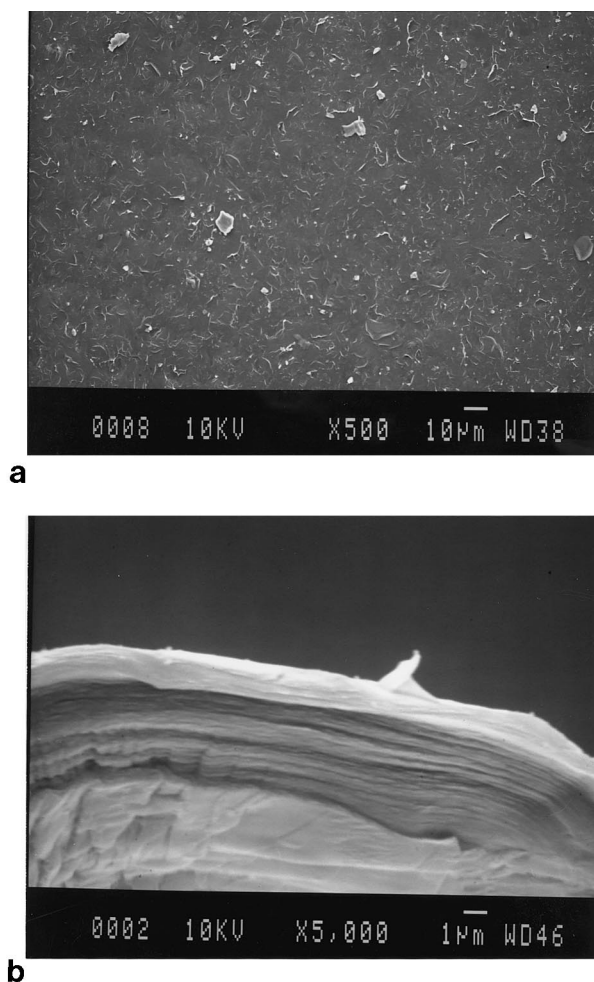


Fig. 5. SEM of: (a) free surface; and (b) fracture surface of cast SPBI film.

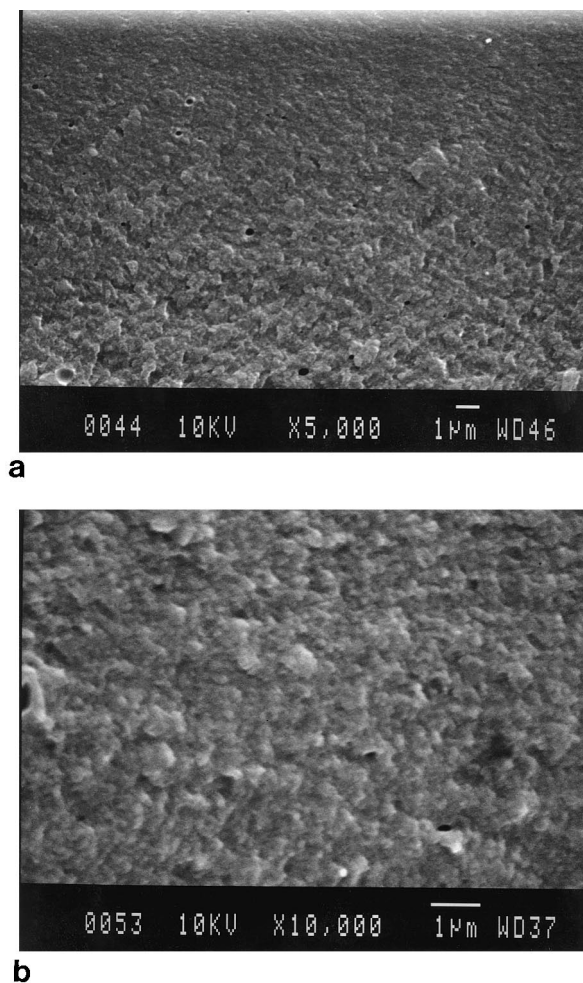


Fig. 6. Fracture surface morphology by SEM of: (a) as cast 10/90 (w/w) SPBI/PVP film; and (b) heat-treated (203°C) 10/90 (w/w) SPBI/PVP film.

current study. The key difference, however, is that the total polymer concentration in our work is above the critical concentration. Even after heating the film to 203°C, close to its  $T_g$  (the  $T_g$  of the compression molded 10/90 SPBI/PVP composite was measured as 210°C from DMA, see Table 3), we see no evidence for phase separation, indicating the tenacity of the interaction between the pyridine and the sulfonic acid groups. Similarly there is no evidence of phase separation in the as cast as well as heat-treated (203°C) 50/50 (w/w) SPBI/PVP film composite, when examined by low voltage, high resolution SEM. It has to be noted, however, in this case, that the heat treatment temperature may be well below the  $T_g$  of the 50/50 SPBI/PVP blend. The fracture morphology is shown in Fig. 7. While no aggregation of the phases is seen, striations ca. 60 nm in width are observed. These are similar to the striations observed in the micrographs of the SPBI homopolymer, indicative of the high rod content. The size of the domains remain unchanged after heat treatment. Hwang et al. [2], however, examined vacuum cast films from a homogeneous solution of PBT/ABPBI (20/80) and found that

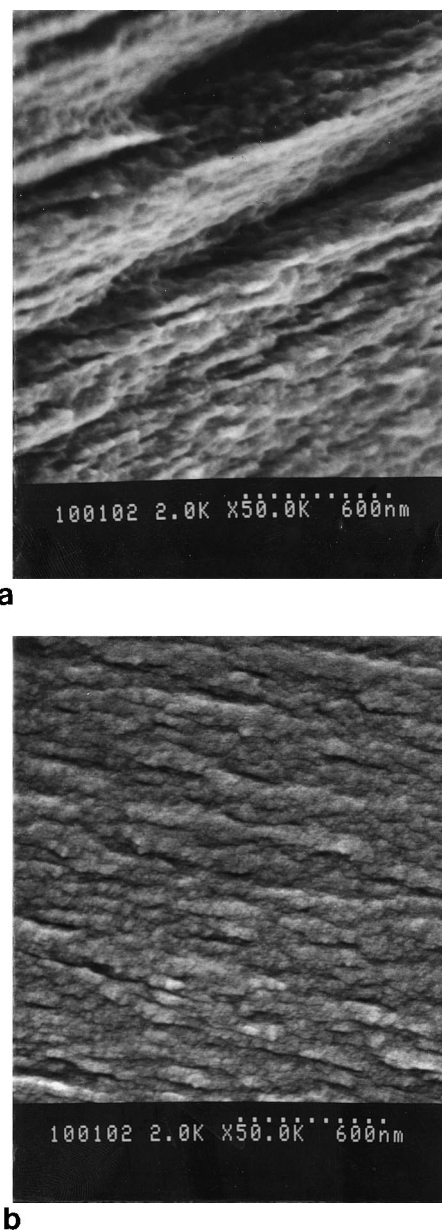


Fig. 7. High resolution SEM of fracture surfaces of: (a) as cast 50/50 (w/w) SPBI/PVP; and (b) heat-treated (203°C) 50/50 (w/w) SPBI/PVP film.

during slow evaporation of the solvent, the concentration of the polymer in solution exceeded the  $C_{cr}$  of the rod, leading to aggregate formation.

Fig. 8 shows SEMs of the fracture surfaces of compression molded molecular composites with compositions of 5/95, 10/90 and 20/80 (w/w) SPBI/PVP. The 5/95 and 10/90 samples were molded at temperatures (210 and 220°C, respectively) sufficiently above the  $T_g$ s of the blend systems (see Table 3), as measured by DMA. The 20/80 (w/w) SPBI/PVP aggregate was compression molded at a temperature of 240°C, however, we could not detect a  $T_g$  for this composition in the DMA experiment. In the case of all the thermally consolidated blends, a very intimate dispersion of the two phases is seen. The micrographs also indicated that good



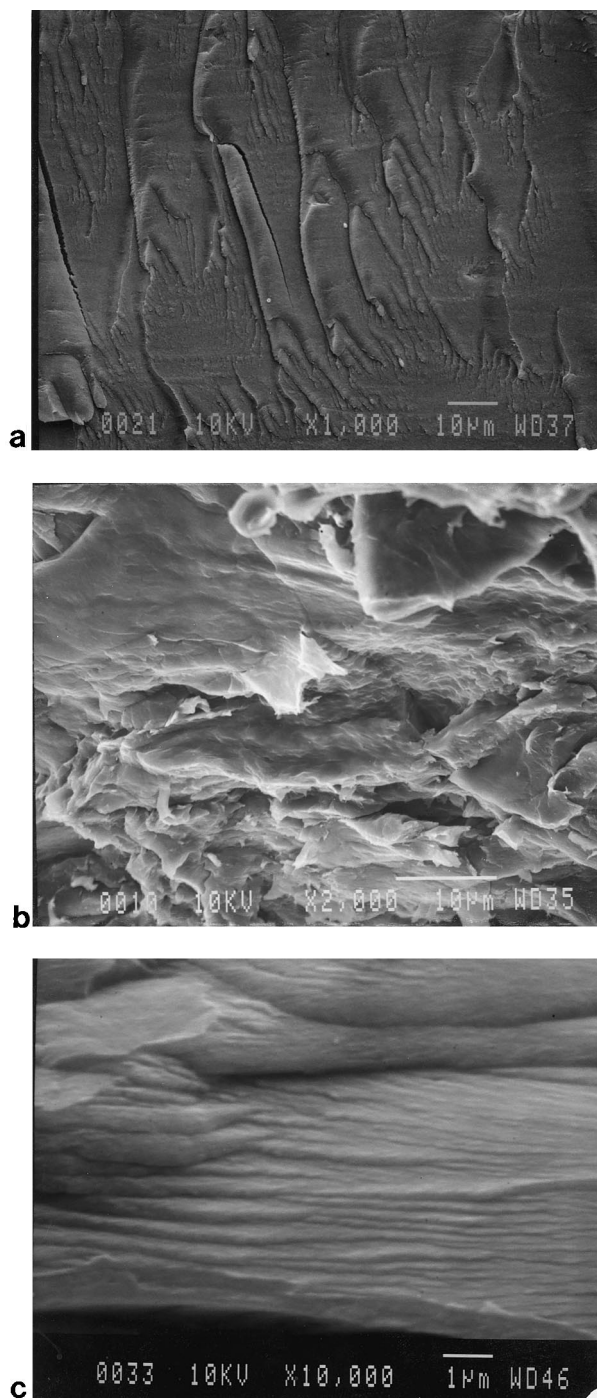


Fig. 8. Fracture surface morphology by SEM of compression molded composites: (a) 5/95 (w/w) SPBI/PVP; (b) 10/90 (w/w) SPBI/PVP; and (c) 20/80 (w/w) SPBI/PVP.

flow and consolidation have occurred. Also, as the content of the rod increases, the failure behavior becomes more ductile in nature, indicative of enhanced fracture toughness. Parker et al. [28,29] have demonstrated that the addition of the anionic poly(*p*-phenyleneterephthalamide) changes the failure behavior of PVP from crazing to shear deformation, accompanied by increases in tensile strength/stiffness and toughness. Although the static mechanical properties of the

SPBI/PVP molecular composites have yet to be evaluated, we should emphasize that the DMA data obtained so far do show a marked increase in  $T_g$  as well as in the storage modulus, as the rod content dispersed in the matrix is increased. It is also important to emphasize the fact that the composites do not phase separate after compression molding indicates enhanced miscibility due to the tenacity of the intermolecular interaction between the individual polymer components.

### 3.3.2. Wide angle X-ray scattering studies

WAXS was utilized to elucidate the microstructure of both SPBI and SPBI/PVP composite films since it probes the structure on a molecular scale and can detect any changes in the unit cell packing that might occur. Previous work on physical blends of PBT and ABPBI [27] and copolymers of articulated rods with thermoplastic pendants [30] have shown characteristic rod-like reflections (when  $C > C_{cr}$  for the physical blends), with these reflections becoming more visible after heating. Examination of the matrix PVP (not shown) showed a broad, amorphous WAXS pattern centered at a  $2\theta$  of  $19.9^\circ$  corresponding to an average d-spacing of  $4.45 \text{ \AA}$ . Fig. 9 shows WAXS patterns for SPBI, taken with the X-ray beam perpendicular (flat view) and parallel (edge view) to the plane of the film. The plots are the results of equatorial scans taken from phosphor image plates. The pattern corresponding to the flat view exhibits a moderate, diffuse peak centered at  $25^\circ$  with a d-spacing of  $3.50 \text{ \AA}$ . It is also noted that three other weak, diffuse rings with d-spacings of  $2.37$ ,  $5.50$  and  $11.33 \text{ \AA}$ , respectively, are visible in the image plate pattern, but not in the digitized pattern. The spacing at  $3.50 \text{ \AA}$  is equal to one of the strong equatorial spacings reported for PBO [31–34], PBT [2,27] and ABPBI [2,27] which has been indexed as 010, corresponding to those planes formed by face to face packing of the molecules. The spacing of  $5.50 \text{ \AA}$  is slightly larger than that of an equivalent reflection reported for PBO, but slightly less than that reported for PBT ( $5.80 \text{ \AA}$ ) [27]. In both those polymers, this reflection has been attributed to those planes formed by side to side packing of the molecules. The other reflection seen is presumably meridional, with the spacing of  $11.33 \text{ \AA}$  lying close to the value of  $11.5 \text{ \AA}$  for ABPBI. This spacing for ABPBI has been attributed to the length of two monomer units of an ABPBI chain in the extended helical chain conformation [2]. The spacing of  $11.33 \text{ \AA}$  that we observe for SPBI presumably corresponds to the length of one monomer repeat unit. It should be noted that until now, no morphological work has been reported on SPBI or PBI, its non-sulfonated analog; attempts to synthesize high molecular weight versions of the latter have been unsuccessful [35].

Comparison of the WAXS pattern taken in the edge view relative to the pattern taken in the flat view (Fig. 9) reveals a marked change in the intensities of reflections seen as well as the presence of additional reflections, indicative of an anisotropic texture in the SPBI film. While similar

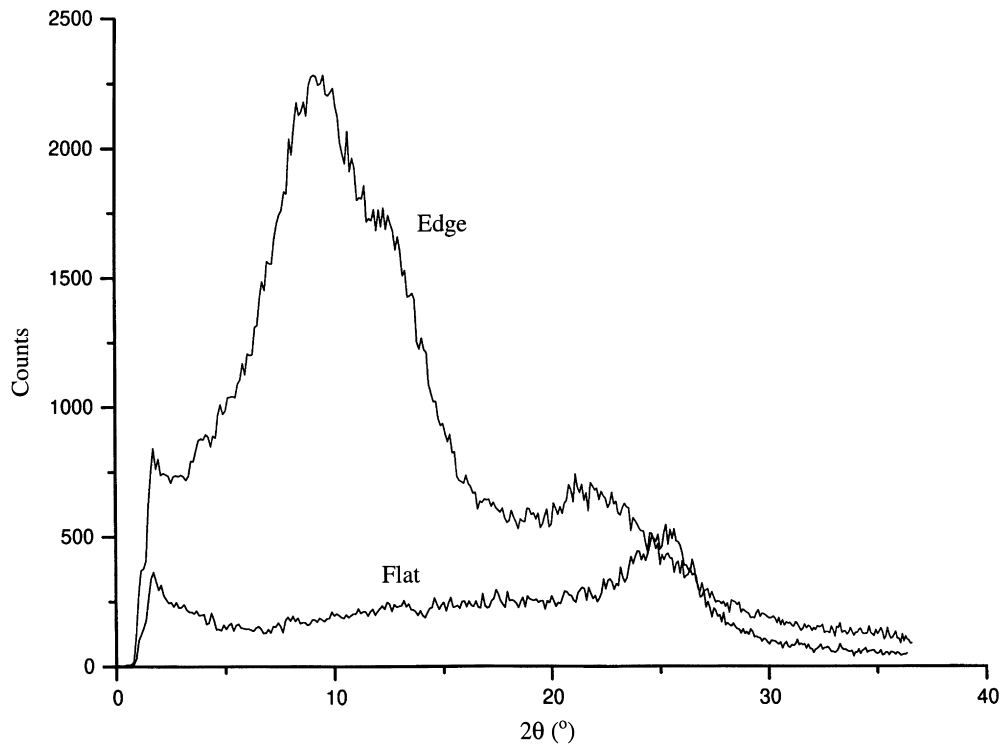


Fig. 9. WAXS traces (flat view and edge view) of cast SPBI film.

anisotropic textures have been reported for sheared films of PBO [26] and BBL, a ladder-like rigid-rod polymer [36], no such textures have been reported for as cast films of these polymers. In both instances, the molecular plane was observed to be perpendicular to the film surface, with the

chain axis being random but lying in the plane of the film surface. We propose a similar phenomenon for SPBI, which, as mentioned earlier, has not been subjected to any shear.

Fig. 10 depicts the WAXS patterns of as cast SPBI/PVP films (50/50 and 10/90, w/w) taken with the beam

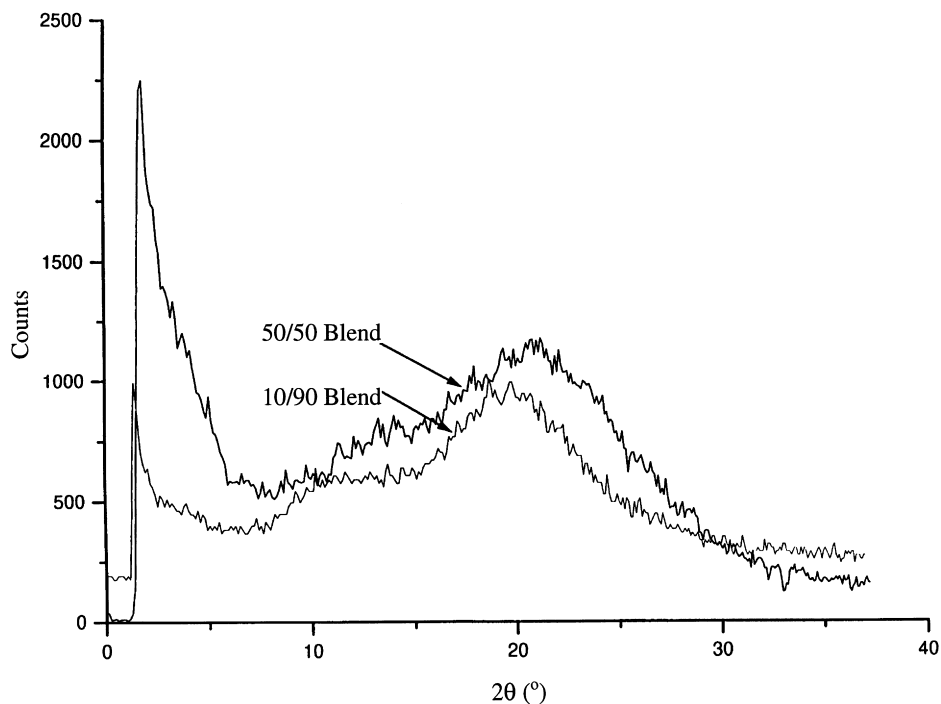


Fig. 10. Flat view WAXS traces of as cast 10/90 (w/w) SPBI/PVP and 50/50 (w/w) SPBI/PVP films.

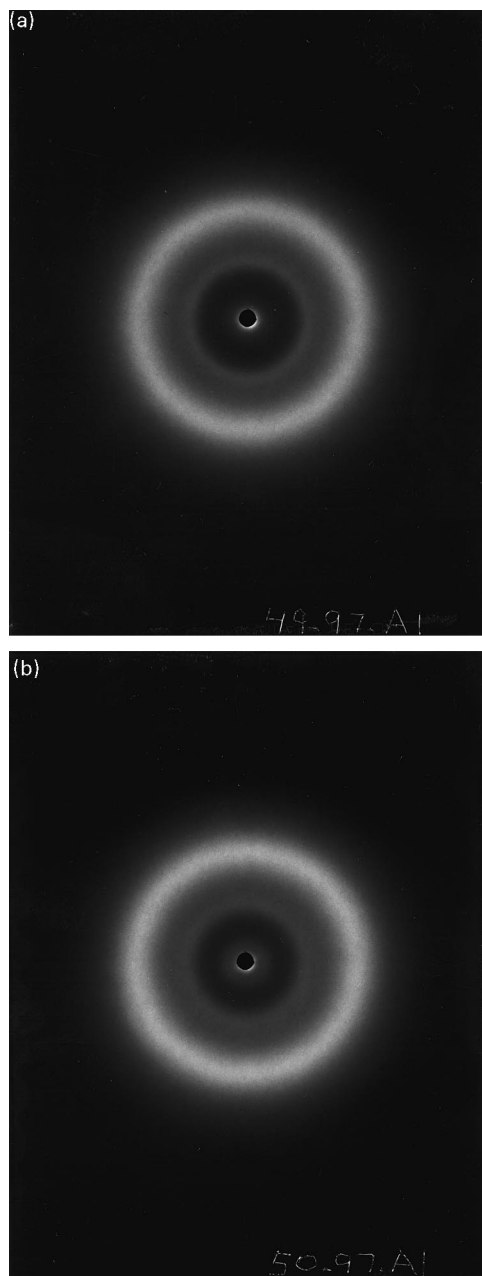


Fig. 11. Flat view WAXS patterns of: (a) as cast; and (b) heat-treated (203°C) 10/90 (w/w) SPBI/PVP films.

perpendicular to the surface (flat view). It can be seen that the diffuse SPBI reflection with a  $d$ -spacing of  $3.50 \text{ \AA}$  is barely visible in the patterns for the molecular composites (the WAXS experiments show very broad, amorphous patterns centered around  $2\theta = 19\text{--}21^\circ$ ), indicating that the small degree of order seen in the pure SPBI has been disrupted even further by the interaction with PVP. Similar observations can be made in the case of the WAXS patterns for 10/90 (w/w) SPBI/PVP and 50/50 (w/w) SPBI/PVP composite films even after heat treatment. As an example, Fig. 11 shows the flat view WAXS photographs of as cast and heat-treated (203°C) 10/90 (w/w) SPBI/PVP film. The

lack of any observable changes, in comparison with the as cast film, in the WAXS pattern upon annealing the composite film close to the  $T_g$  of the blend indicates that the acid–base interactions between the rod and the coil polymer components suppress the tendency for rod aggregation in contrast to the physical blends of PBT and ABPBI [27].

### 3.3.3. Small angle X-ray scattering

In the case of both as cast and heat-treated composite films as well as the compression molded composites, corroborative evidence for homogeneity and miscibility were obtained from SAXS. SAXS probes the microstructure on the scale of 1–200 nm [37] and provides information regarding the electron density distribution of the material. Analysis of the angular distribution of the peak intensities (if there are peaks) reveals the periodicity and magnitude of that electron density distribution. The principle is that X-rays are scattered by regions of varied electron density such as voids, polymer lamellae or phase separated domains and the intensity is related to the number and contrast of these regions. Fig. 12 delineates the SAXS patterns for as cast and heat-treated 50/50 (w/w) SPBI/PVP molecular composite films as well as a compression molded 20/80 (w/w) SPBI/PVP sample. In all cases, no scattering characteristic of differences in electron density attributable to the presence of phase separated domains is observed. The SAXS findings are consistent with those derived from the SEM studies on as cast and heat-treated SPBI/PVP molecular composite films as well as compression molded SPBI/PVP composites. This indicates that in all the composite samples examined, the rod molecules are well dispersed in the polar amorphous matrix coil. It is also evident from the example of the compression molded composite that thermal consolidation of the rod/coil blend has not resulted in any observable phase separation [38]. This is in contrast to the thermally induced phase separation of the rigid-rod during consolidation of rod-thermoplastic polymers in various PBT/thermoplastic composites investigated so far [4–6].

### 3.4. Morphology of as cast and cured thermoset rigid-rod film composites

Both the SPBI/nadimide thermoset and SPBI/benzoxazine thermoset composite films were thermally cured at 250°C for 1 h under a flow of dry nitrogen. The dispersion of the rigid-rod polymer in the thermoset matrix in both as cast and cured film composites were examined by SEM and SAXS. The fracture morphology of the as cast as well as thermally cured 42/58 (w/w) SPBI/nadimide thermoset film as delineated by SEM (Fig. 13) does not show any phase separated domains and demonstrates very good dispersion of the rigid-rod in the thermoset matrix. Similarly, fracture morphology by SEM of the as cast and thermally cured molecular composite films of SPBI and the benzoxazine thermosetting system (48/52 (w/w) rod/thermoset)

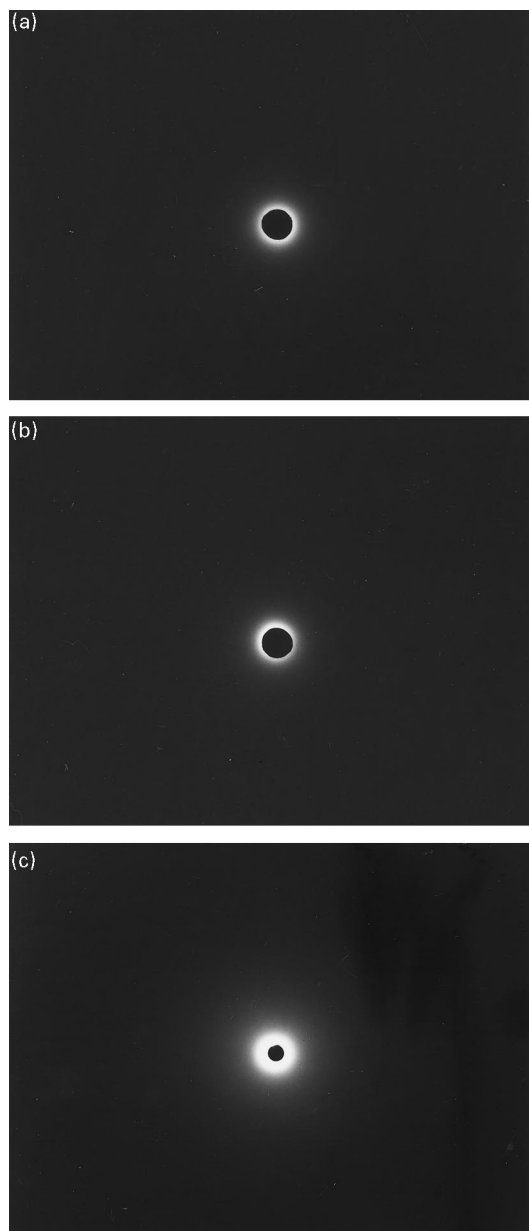


Fig. 12. SAXS patterns of: (a) as cast; (b) heat-treated 50/50 (w/w) SPBI/PVP molecular composite film; and (c) compression molded 20/80 SPBI/PVP composite.

(Fig. 14) shows no phase separated domains in the composite. The lack of any observable changes in the microstructure even after curing, is indicative of a highly miscible system [39]. This also seems to indicate that the observed microstructure is indeed an equilibrium microstructure where the high level of miscibility is attributable to the negative enthalpy of the acid–base interaction between the polymer components.

The SAXS examination of the thermoset molecular composites further validated the SEM observations. An example for SAXS is shown for the cured films of 48/52 (w/w) SPBI/benzoxazine as well as 42/58 (w/w) SPBI/nadimide thermoset molecular composites (Fig. 15). No coherent

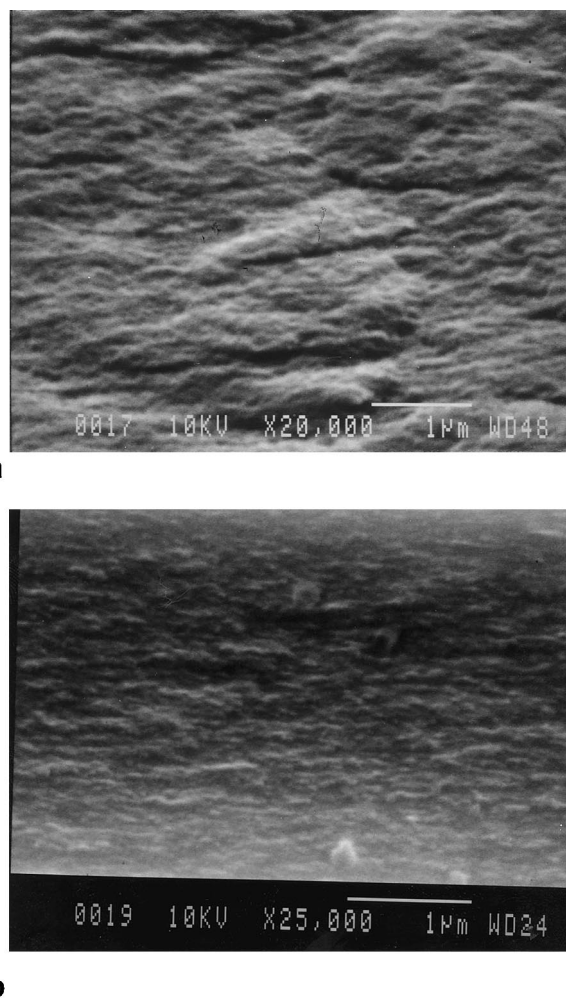


Fig. 13. Fracture morphology by SEM of: (a) as cast; and (b) thermally cured 42/58 (w/w) SPBI/nadimide thermoset molecular composite film.

scattering is seen in the SAXS pattern. This indicates a homogenous microstructure and points to the miscibility of the rod and the matrix phases with no detectable phase separated domains in the range probed by this technique.

#### 4. Summary and conclusions

A novel method of processing solvent cast aromatic heterocyclic rigid-rod thermoplastic as well as thermoset matrix molecular composites above the  $C_{cr}$  of the rigid-rod polymer in solution, with no occurrence of phase separation, is demonstrated. Blend miscibility of the rod (sulfonic acid-pendent poly(*p*-phenylenebenzobisimidazole), SPBI) and the basic thermoplastic matrix (poly(4-vinylpyridine) (PVP) and poly(2-vinylpyridine)) or the basic thermoset monomers with phenylethynyl, nadimide and bisbenzoxazine functionalities was facilitated by acid–base interaction between the rigid-rod and the thermoplastic or thermoset host. The blends were compatibilized and solvent cast via the mechanism of ionic interchange between

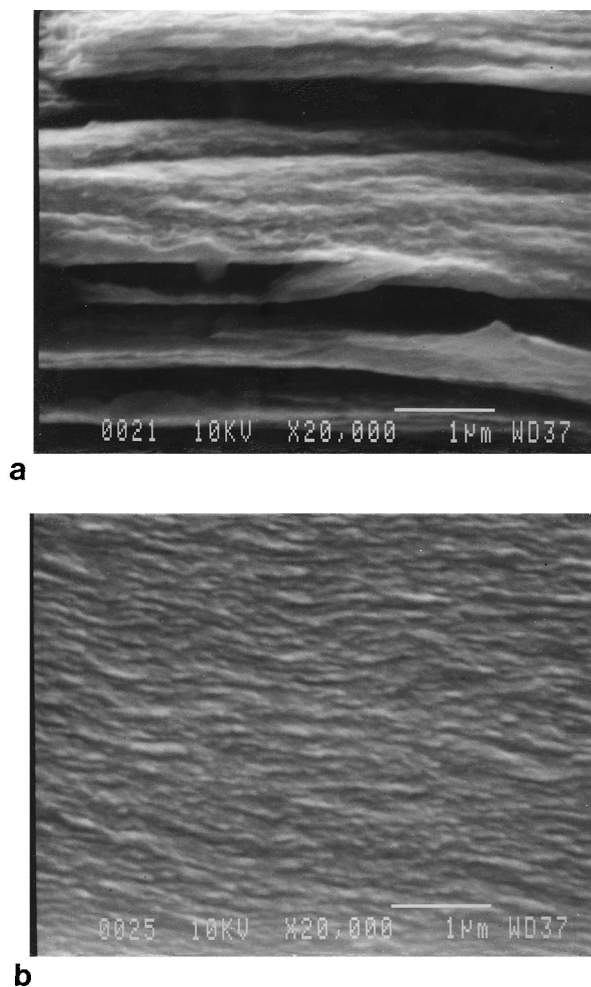


Fig. 14. Fracture morphology by SEM of: (a) as cast; and (b) thermally cured 48/52 (w/w) SPBI/benzoxazine thermoset molecular composite film.

alcohol-solubilized triethylammonium salt of SPBI and the basic thermoplastic or thermoset host. Homogeneous, optically transparent film composites were obtained with miscibility over a wide range of compositions.

An SEM examination of as cast and heat-treated SPBI/PVP molecular composite films revealed a homogeneous microstructure with no observable domains due to phase separation. The fine level of dispersion of the rigid-rod molecules in the polar amorphous matrix was also corroborated by WAXS flat view patterns and SAXS evidence. The lack of any observable microstructural evidence for phase separation in compression molded composites indicates enhanced miscibility due to the tenacity of acid–base interaction between the rigid-rod and the coiled matrix. Similar conclusions with regard to the high level of miscibility of the dispersed and the matrix phases can be drawn from the SEM and SAXS investigations of the as cast and the thermally cured rigid-rod thermoset composite films.

Preliminary DMA studies revealed a significant enhancement of the  $T_g$  as well as the storage modulus, relative to the pure thermoplastic matrix, of a thermally consolidated

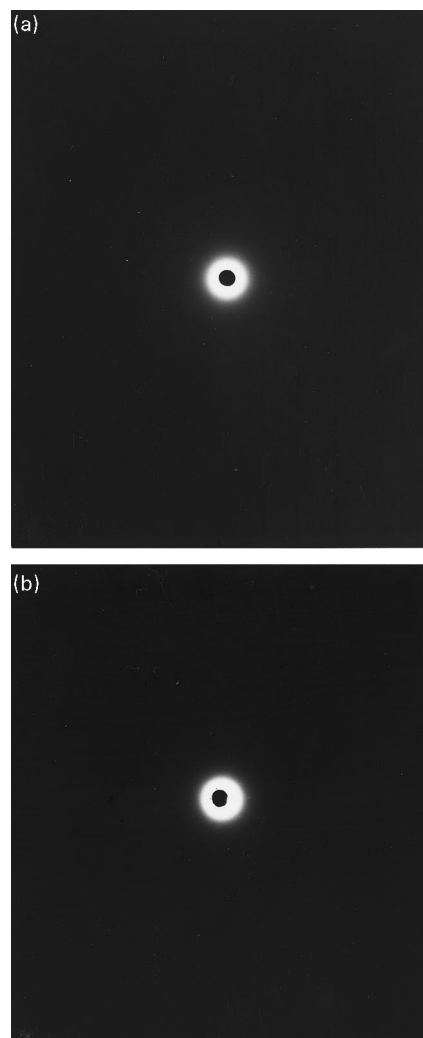


Fig. 15. SAXS patterns of: (a) thermally cured 48/52 (w/w) SPBI/benzoxazine thermoset molecular composite film; and (b) thermally cured 42/58 (w/w) SPBI/nadimide thermoset molecular composite film.

composite with as little as 5 wt% incorporation of the rod in the amorphous matrix. Such an enhancement in thermo-mechanical properties is attributable to the synergism arising from the specific interaction between the interacting polymer components in the blend.

## References

- [1] Helminiak TE, Benner CL, Husman GE, Arnold FE. US Patent 1980;4,207, 407.
- [2] Hwang WF, Wiff DR, Benner CL, Helminiak TE. J Macromol Sci Phys 1983;22(2):231.
- [3] Hwang WF, Wiff DR, Verchoore C. Polym Engng Sci 1983;23:790.
- [4] Wang CS, Goldfarb IJ, Helminiak TE. Polymer 1988;29:825.
- [5] Hwang WF, Wiff DR, Helminiak TE, Adams WW. Org Coat Appl Polym Sci Proc Am Chem Soc 1983;48:919.
- [6] Arnold Jr. FE, Arnold FE. Advances in polymer science, high performance polymers, 117. Berlin: Springer, 1994. p. 257.
- [7] So Y-H, Sen A, Kim P, Jeor VSt. J Polym Sci Polym Chem 1995;33:2893.

- [8] Chuah HH, Tan L-S, Arnold FE. *Polym Engng Sci* 1989;29(2):107.
- [9] Tan L-S, Venkatasubramanian N. *J Polym Sci Polym Chem* 1996;34:3539.
- [10] Wang CS, Venkatasubramanian N, Price GE, Houtz M, Tan L-S. *Polym Prepr* 1995;36(2):247.
- [11] Eisenbach CD, Hofmann J, MacKnight WJ. *Macromolecules* 1994;27:3162.
- [12] Eisenbach CD, Fischer K, Hofmann J, MacKnight WJ. *J Macromol Symp* 1995;100:105.
- [13] Parker G, Chen W, Hara M. *Polym Mater Sci Eng* 1995;72:544.
- [14] Chen W, Hara M. *Polym Prepr* 1996;37(1):388.
- [15] Tan L-S, Arnold FE, Chuah HH. *Polymer* 1991;32(8):1376.
- [16] Dang TD, Arnold FE. *Mater Res Soc Symp Proc* 1993;305:49.
- [17] Dang TD, Chen JP, Arnold FE. *US Patents* 1996;5,492, 996; 5,508, 376.
- [18] Premachandra J, Kumidinie C, Zhao W, Mark JE, Dang TD, Chen JP, Arnold FE. *J Sol–Gel Sci Technol* 1996;7:163.
- [19] Tan L-S, Arnold FE. *Polym Prepr* 1991;32(1):51.
- [20] Ning X, Ishida H. *J Polym Sci Polym Chem* 1994;32:1121.
- [21] Ning X, Ishida H. *J Polym Sci Polym Phys* 1994;32:921.
- [22] Parker G, Hara M. *Polymer* 1997;38(11):2773.
- [23] Kaplan DS. *J Appl Polym Sci* 1976;20:2615.
- [24] Utracki LA. *Polymer alloys and blends: thermodynamics and rheology*, New York: Hanser Publishers, 1990.
- [25] Dang TD, Bai SJ, Heberer DP, Arnold FE, Spry RJ. *J Polym Sci Polym Phys* 1993;31:1941.
- [26] Dean DR, Husband DM, Dotrong M, Wang CS, Dotrong MH, Click W, Evers RC. *J Polym Sci Polym Chem* 1997;35:3457.
- [27] Krause SJ, Haddock T, Price GE, Lenhart PG, O'Brien JF, Helminiak TE, Adams WW. *J Polym Sci Polym Phys* 1986;24:1991.
- [28] Parker G, Hara M. *Polymer* 1997;38(11):2701.
- [29] Parker G, Chen W, Tsou L, Hara M. In: Isayev AI, Kyu T, Cheng SZD, editors. *Liquid-crystalline polymer systems—technological advances*, ACS Symposium Series, 632. American Chemical Society, 1996. p. 54.
- [30] Bai SJ, Dotrong M, Evers RC. *J Polym Sci Polym Phys* 1992;30:1515.
- [31] Wang CS, Bai SJ, Rice BP. *Polym Mater Sci Eng* 1989;61:550.
- [32] Krause SJ, Haddock T, Vezie D, Lenhart PG, Hwang WF, Price GE, Helminiak TE, O'Brien JF, Adams WW. *Polymer* 1988;29:1354.
- [33] Martin DC, Thomas EL. *Macromolecules* 1991;24:9.
- [34] Kumar S, Warner S, Grubb DT, Adams WW. *Polymer* 1994;35:5408.
- [35] Dang TD, Arnold FE. Unpublished work.
- [36] Song HH, Fratini A, Chabinye M, Price GE, Agrawal A, Wang CS, Burkett J, Dudis D, Arnold FE. *Synth Metals* 1995;69:533.
- [37] Sawyer LC, Grubb DT. *Polymer microscopy*, London: Chapman and Hall, 1996.
- [38] Venkatasubramanian N, Dang TD, Dean DR, Price GE, Arnold FE. *Polym Prepr* 1997;38(2):303.
- [39] Dang TD, Venkatasubramanian N, Dean DR, Price GE, Arnold FE. *Polym Prepr* 1997;38(2):301.